Study of Bunch Instabilities by the Nonlinear Vlasov-Fokker-Planck Equation

Robert L. Warnock

Stanford Linear Accelerator Center, Stanford University
*P.O. Box 20450, Stanford, CA, U.S.A.*

e-mail: warnock@slac.stanford.edu

Abstract. Instabilities of the bunch form in storage rings may be induced through the wake field arising from corrugations in the vacuum chamber, or from the wake and precursor fields due to coherent synchrotron radiation (CSR). For over forty years the linearized Vlasov equation has been applied to calculate the threshold in current for an instability, and the initial growth rate. Increasing interest in nonlinear aspects of the motion has led to numerical solutions of the nonlinear Vlasov equation, augmented with Fokker-Planck terms to describe incoherent synchrotron radiation in the case of electron storage rings. This opens the door to much deeper studies of coherent instabilities, revealing a rich variety of nonlinear phenomena. Recent work on this topic by the author and collaborators is reviewed.

INTRODUCTION

I will concentrate on longitudinal motion of electrons in a storage ring, the phase space coordinate being the longitudinal distance of a particle from a reference particle which circulates on an ideal orbit with energy E_0; the conjugate momentum is the deviation of the particle's energy from E_0. With appropriate modifications the general approach should apply as well to transverse motion, and also to particles such as protons which emit relatively little synchrotron radiation.

At low beam current a bunched electron beam in a storage ring has a nearly Gaussian particle distribution, thanks to equilibration due to damping and diffusion from random emission of synchrotron radiation in quanta. At higher current there are deviations from the Gaussian form due to interaction of the bunch with its electromagnetic environment: fields excited by the beam in various corrugations of the metallic vacuum chamber (cavities, bellows, transitions, etc.) act back on the beam so as to modify the potential well of the external r.f. field. This self-field mediated by the vacuum chamber is called the "machine wake field". It provides a feedback loop that typically becomes unstable at some threshold in beam current, giving an initial exponential growth of some small perturbation of the equilibrium bunch form. The instability is expected to saturate, which is to say that unlimited growth is suppressed by nonlinear effects. Saturation may allow one to operate the machine above threshold, but that possibility depends on the exact pattern of bunch behavior at high current. Thus, there
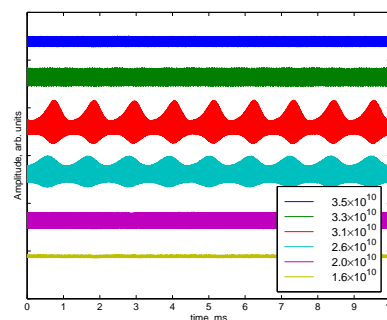

FIGURE 1. Sawtooth mode in SLC damping ring. Oscilloscope trace of BPM signal followed by square-law detector, several traces for current increasing, bottom to top

is a strong motivation to predict and analyze nonlinear effects. An example of the interesting phenomena that arise in the nonlinear, high-current regime is the sawtooth mode, in which the bunch length undergoes oscillations of quadrupole type with slowly varying amplitude, the amplitude changing periodically with period comparable to the damping time of the ring. Figure 1 shows an observation of the sawtooth in the SLC damping ring.

Another aspect of the self-field of a bunch arises from centripetal acceleration on curved trajectories, giving synchrotron radiation. Components of the radiation with wavelength comparable to the bunch size or larger may come from all particles in the bunch radiating coherently, as though they formed a continuous charge/current
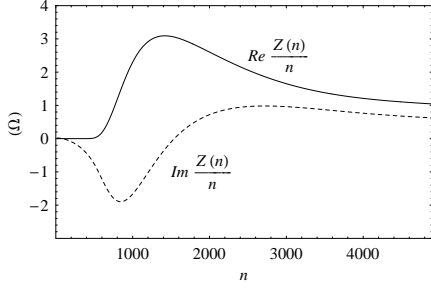
FIGURE 2. Real and imaginary parts of $Z(n)/n$ in ohms, where n/R is the wave number. Parallel-plate model with $h = 4.2$ cm, $R = 1.9$ m, and $E_0 = 737$ MeV, parameters appropriate for NSLS-VUV ring.
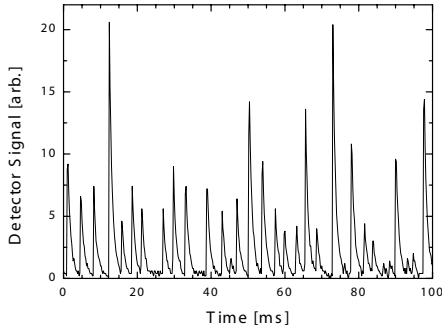
FIGURE 3. Far infrared detector output at NSLS VUV (Courtesy of G. Carr). Damping time $\tau_\varepsilon = 7$ ms

source. The power from this CSR is proportional to N^2, the number of particles squared, whereas power from incoherent radiation goes as N. Consequently, CSR contributes an intense self-field, with wake and precursor components, which is a potential source of bunch instability beyond the effect of the machine wake.

Fortunately, CSR appears only in special circumstances, thanks to so-called "shielding" due to the vacuum chamber. The chamber provides an exponential suppression of CSR with wavelength greater than the shielding cutoff λ_0, where an estimate from a simple model of the vacuum chamber (infinite parallel plates with separation h) gives $\lambda_0 \approx 2h\sqrt{h/R}$, for bending radius R. Figure 2 shows the cutoff in the real part of the radiation impedance at long wavelength, thus a cutoff in radiated power which is proportional to Re$Z(n)$.

In normal electron rings, λ_0 is small compared to the bunch length, which seems to indicate that CSR would be suppressed. If, on the other hand, the bunch shows micro-bunching (significant Fourier components of wavelength much less than the bunch length), then there can be substantial coherent radiation. Micro-bunching may arise through an instability at high current, perhaps due to the CSR field itself, alone or in combination with the

machine wake. Experimental evidence of this effect has appeared at several light source rings in recent years. As we shall see, the conditions for micro-bunching are transitory, but reappear in a roughly periodic manner, with period comparable to the longitudinal damping time of the ring. Thus we have CSR appearing in bursts, as in data from the NSLS-VUV ring shown in Figure 3.

The traditional tool to determine the threshold of instability is the Vlasov equation, linearized about the equilibrium distribution (or some approximation of the equilibrium). In the case of a coasting beam (no imposed r.f. field) this theory closely resembles Landau's original treatment of plasma oscillations [1]. One tries, with some success, to apply the coasting beam theory also to the bunched beam, usually the case of practical importance. I wish to argue that the full nonlinear Vlasov equation, augmented to include Fokker-Planck terms to account for incoherent synchrotron radiation, provides a good basis for theory and numerical simulation of multiparticle beam dynamics in a range of accelerator problems. It is more common to apply the macro-particle method in simulations, perhaps because the required coding is perceived to be simpler. In examples with a two-dimensional phase space, I will show that the coding required for a Vlasov-Fokker-Planck (VFP) simulation is in fact very simple, and that spurious noise is much lower than in the macroparticle approach. In higher dimensions the macroparticle method seems to be more practical than current versions of VFP solvers. Efforts to extend the success of the VFP method to higher dimensions are underway, and should have a high priority in further work.

I will review work carried out during the past six years, mostly in collaboration with Jim Ellison and Marco Venturini. Several other people made important contributions to our efforts: Karl Bane, Ron Ruth, Gennady Stupakov, Fernando Sannibale, Gabriele Bassi, King-Yuen Ng, Mathias Vogt, Andrey Sobol, and Marc Salas.

VLASOV-FOKKER-PLANCK EQUATION

Our dimensionless phase space variables (q, p) and time coordinate τ are as follows:

$$q = \frac{z}{\sigma_z} , \quad p = -\text{sgn}\,(\eta)\frac{E - E_0}{\sigma_E} , \quad \tau = \omega_s t$$

$z = $ distance from reference particle, > 0 in front

$E = $ energy , $E_0 = $ design energy

$\omega_s = $ synchrotron frequency

$$\eta = \text{slip factor}, > 0 \text{ above transition}$$

Here σ_z and σ_E are any scale factors such that

$$\frac{\beta_0 \omega_s \sigma_z}{c} = \frac{|\eta| \sigma_E}{E_0} , \qquad (1)$$

$\beta_0 c$ being the velocity for energy E_0. The single-particle phase space density is denoted by $f(q, p, \tau)$. It has unit integral, $\int f(q, p, \tau) dq dp = 1$. The VFP equation in the form that we apply is [2]

$$\frac{\partial f}{\partial \tau} + p \frac{\partial f}{\partial q} - [q + I_c F(q, f, \tau)] \frac{\partial f}{\partial p} =$$
$$\frac{2}{\omega_s t_d} \frac{\partial}{\partial p} \left(pf + \frac{\partial f}{\partial p} \right), \qquad (2)$$

where $-q$ is the harmonic restoring force from the r.f., and $-I_c F(q, f, \tau)$ is the longitudinal coherent force determined by Maxwell's equations with charge/current sources as obtained from f itself. The normalized beam current is I_c, and t_d is the damping time. The terms on the right hand side give the Fokker-Planck account of damping and diffusion from incoherent emission of synchrotron radiation in quanta. The damping and diffusion constants happen to be equal with our choice of variables.

Following usual practice, we represent the coherent force in terms of a wake potential $W(q)$, as follows:

$$F(q, f, \tau) = \int W(q - q') \rho(q', \tau) dq' , \qquad (3)$$

$$\rho(q, \tau) = \int f(q, p, \tau) dp . \qquad (4)$$

Here $W(q - q')$ is the longitudinal electric field at q due to a point source at q', averaged over one turn. In practice the machine wake potential is computed by solving Maxwell's equations with a short Gaussian bunch rather than a point charge as source. Since (3) depends only on the current value of the particle density ρ, certain retardation effects are neglected. The latter may have some importance in the case of CSR [3]. For CSR we compute F from the impedance (Fourier transform of W) in the parallel plate model. Since W for CSR is rapidly varying, it is difficult to deal with it numerically.

EQUILIBRIUM SOLUTION AND LINEARIZATION

The equilibrium solution of the VFP equation is used in two ways: first, we compute the threshold of instability by linearizing the Vlasov equation about the equilibrium; second, we use the equilibrium solution as the starting point for a time domain integration of the nonlinear VFP.
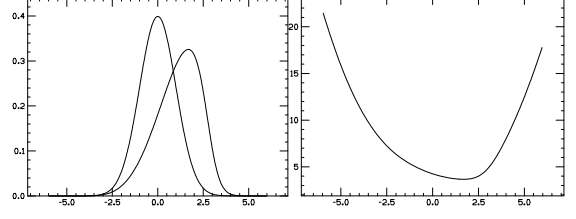
FIGURE 4. Equilibrium particle distribution (compared to unperturbed Gaussian) and distorted potential well for SLC damping ring with bunch population $N = 3.2 \cdot 10^{10}$.

This latter can be used to confirm the threshold obtained from linearization, or merely to provide a quiet start for the integration even when the current is well above threshold.

A distribution of the form

$$f_0(q, p) = \frac{e^{-p^2/2}}{\sqrt{2\pi}} \rho(q) \qquad (5)$$

is a time-independent solution of (2) provided that ρ solves the Haïssinski integral equation,

$$\rho(q) = \frac{e^{-H(q, \rho)}}{\int e^{-H(r, \rho)} dr} , \qquad (6)$$

where H is the "self-consistent Hamiltonian" or "distorted potential well",

$$H(q, \rho) = q^2/2 - I_c \int S(q - r) \rho(r) dr ,$$
$$S(q) = \int_q^\infty W(r) dr . \qquad (7)$$

At small enough current, the solution of the Haïssinski equation is unique in a certain space, for a wide class of W. That follows easily from the contraction mapping theorem.

For a numerical solution of (6) we discretize the integrals by some quadrature rule, thus obtaining a system of algebraic equations for the values of ρ at mesh points. A solution of those equations by Newton's method, with the unperturbed Gaussian as a first guess, proves to be very fast and robust at typical currents. For extremely high current (say ten times a realistic current), one still gets a solution by using a linear extrapolation of a solution at lower current as the first guess. Note that the normalization integral in (6) is part of the functional equation, so that a solution is automatically normalized. Figure 4 shows a typical Haïssinski solution and the corresponding distorted potential well.

To determine the threshold of an instability including the case of a bunched beam, we drop the Fokker-Planck terms and linearize the resulting Vlasov equation about

the equilibrium solution. Dropping the FP terms is probably a good approximation, since at a current just slightly above threshold the growth rate of a perturbation is so fast that the FP terms do not have time to act; they are effective over times comparable to the damping time, usually in the millisecond range. As in Landau theory, we make a Laplace transform in time. We write the Laplace variable conjugate to time as $p = -i\omega$, and work with the complex frequency ω instead of p. Following Oide and Yokoya [4], we transform to action-angle variables (J, ϕ) of the distorted potential well, and make a Fourier analysis in ϕ. Then a perturbation to an equilibrium, call it $\hat{f}_1(J, m, \omega)$ with Fourier mode number m, satisfies a linear integral equation, essentially the equation of Oide-Yokoya (although those authors made a Fourier transform in time, which need not exist, rather than the Laplace transform which exists for sufficiently large Im ω). Unfortunately, the integral equation is singular, a so-called integral equation of the third kind [5], which has generalized function solutions of the type (Cauchy principal value)+ (delta function), analogous to Case - van Kampen modes of plasma theory. Since these generalized functions cannot be represented numerically, a direct numerical treatment of such an equation will fail to converge under mesh refinement. In practice Oide's code for such a treatment sometimes gives approximate values for thresholds, but often gives ambiguous answers. A better approach is to cast the equation in a form which is non-singular from the viewpoint of operator theory. This can be done simply by redefining the unknown function [6], giving an equation of the form

$$g(m, J, \omega) - ie^{J/2}\check{f}_1(m, J, 0)$$
$$+ \sum_{m'=-\infty}^{\infty} \int_0^{\infty} dJ' \frac{H(m, J, m', J')g(m', J', \omega)}{\omega - m'\Omega(J')} = 0$$

$$\tag{8}$$

where

$$g(m, J, \omega) = e^{J/2}(\omega - m\Omega(J))\hat{f}_1(m, J, \omega) . \tag{9}$$

Here $\Omega(J)$ is the amplitude-dependent frequency for oscillations in the distorted potential well, H is a kernel determined by the wake potential, and $\check{f}_1$ is an initial-value term. Eq. (8) is a regular Fredholm equation for Im $\omega > 0$, but is also well-behaved as Im $\omega \to 0+$ if we define the integral over a pole where $\omega = m'\Omega(J')$ by the usual Plemelj rule [7] $(P(1/x) - i\pi\delta(x))$. In a space of functions $g(m, J)$ with good decay in m and J at infinity, and some smoothness in J (say Hölder continuity), the integral operator is well-behaved (compact), thanks to good decay of $H(m, J, m', J')$ in all variables and its smoothness in J, J'. Consequently, the integral operator can be discretized and approximated numerically. The determinant of the discretized system, $D(\omega)$, determines

4

2

0

−2

−4

−4   −2   0   2   4

J cos(ϕ)

J sin(ϕ)
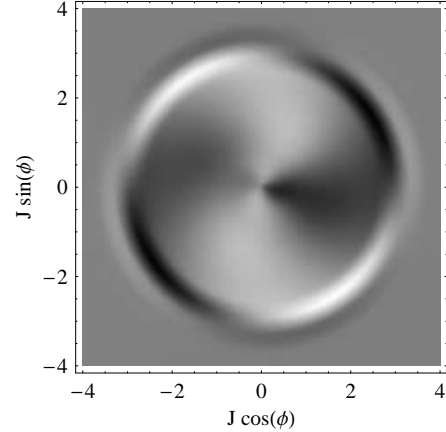
FIGURE 5. Density plot of $f_1(\phi, J)$, the unstable mode for $I_c = 0.048$ with frequency $\omega = 1.860 + i2.311 \times 10^{-3}$.

stability, in exact analogy to the dispersion function of coasting beam theory. A zero of D in the upper half plane means instability. For small current there is no such zero, and the first zero to enter as the current is increased corresponds to the most unstable mode. The distribution function of the mode is obtained by solving the homogeneous equation at the zero of the determinant.

The determinant has zeros corresponding to coherent modes only, none corresponding to the incoherent spectrum of single particle motion where $\omega = m\Omega(J)$. By contrast, eigenvalues in the incoherent spectrum enter the Oide-Yokoya formalism, and are responsible for numerical difficulties since they represent the support of generalized functions.

We have applied (8) to find the threshold of instability in the SLC damping ring, and find good agreement with the threshold determined by time-domain integration of the VFP equation [6]. Figure 5 shows a density plot of the most unstable mode, which is primarily of quadrupole character. For convenience the calculation was done with ω having a small imaginary part.

METHOD FOR SOLUTION OF THE NONLINEAR VFP EQUATION

We write the VFP equation as

$$\frac{\partial f}{\partial \tau} = A_V(f) + A_{FP}(f) . \tag{10}$$

and consider separately the Vlasov (V) and Fokker-Planck (FP) parts of the right hand side. Since A_V and A_{FP} require completely different numerical methods, we employ operator splitting, interleaving small time steps $\Delta\tau$ by A_V alone with steps by A_{FP} alone. This is justified if $\Delta\tau$ is sufficiently small. The FP step is simple and

quick: discretize $\partial/\partial p$ by divided differences and take an Euler step in τ. See [2] for the particular divided difference scheme that is used. Because of the small damping constant, implicit time stepping is not required. The V step is unstable if done by divided differences. Instead we use an approximation to the *method of characteristics*, which proves to be extremely stable.

We suppose that the coherent force is nearly independent of time over a small time interval $\Delta\tau$, so that we have a single-particle map defined locally in time. This volume preserving map is denoted by $M_{\tau\rightarrow\tau+\Delta\tau}(z)$, $z = (q, p)$. Then the Perron-Frobenius (PF) operator $\mathscr{M}$ associated with M gives the time evolution of f:

$$f(z, \tau + \Delta\tau) = \mathscr{M}f(z, \tau) = f(M^{-1}(z), \tau). \qquad (11)$$

This is another way of stating that the number of particles in a phase space volume element dz is preserved:

$$f(M(z), \tau + \Delta\tau)d(M(z)) = f(z, \tau)dz. \qquad (12)$$

A discretization of $\mathscr{M}$ simply consists of choosing a finite-dimensional approximation of f. For instance, f might be described by its values on a grid $\{z_i\}$, with polynomial interpolation to off-grid points. In that case, evaluation of $\mathscr{M}f(z_i, \tau)$ would be done by interpolation, since $M^{-1}(z_i)$ is an off-grid point in general.

We usually refer to this procedure as the PF method, but *method of local characteristics* is more descriptive. In literature on plasmas and fluids [8, 9] it often called the *semi-Lagrangian method*. In plasma physics it dates back at least to the work of Cheng and Knorr [10]. Besides the applications reviewed below, there have been applications to the coherent beam-beam interaction through coupled VFP equations [11, 12, 13], to bunch stretching through harmonic cavities [14], and to problems in beam dynamics with stochastic applied fields [15].

SAWTOOTH MODE IN THE SLC DAMPING RING

We wish to simulate longitudinal beam dynamics in the positron damping ring at the SLC, comparing results to data of Podobedov and Siemann [16]. For typical machine parameters see p.54 of [16], and for details of the calculation see [2]. We apply the wake potential calculated by Karl Bane, who used detailed engineering plans and codes such as MAFIA. Because of difficulties in handling certain three-dimensional structures, and limitations on the length of the driving bunch, the wake potential is not expected to be reliable at very short wavelengths. The PF method was carried out using a 400×400 grid in phase space, and a simple bi-quadratic interpolation to define the distribution function at off-grid points. The number of time steps per synchrotron

period was 1024. The realistic value of the damping time was used ($t_d = 200$ synchrotron periods), and the distribution function was followed for several damping times. The starting distribution function was the Haïssinski equilibrium.

Figure 6 shows the normalized energy spread (variance of p) versus time, for three ascending values of current. At $N = 1.55 \cdot 10^{10}$ we have rather accurate preser-
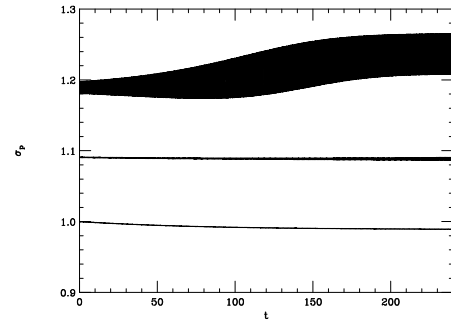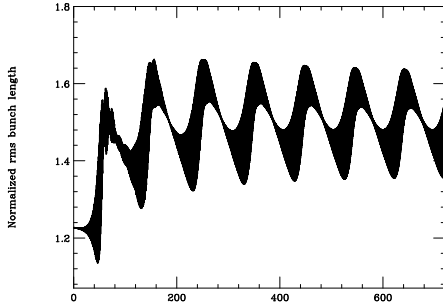

FIGURE 6. Time evolution of the dimensionless energy spread σ_p, for bunch populations $N = (1.55, 1.64, 1.74) \cdot 10^{10}$. The initial value is $\sigma_p = 1$ for each, but to separate the curves we have plotted $\sigma_p(1.55)$, $\sigma_p(1.64) + 0.09$, $\sigma_p(1.74) + 0.18$. The time unit is one synchrotron period. The black band arises by fill-in from rapid oscillations, with frequency close to $2\omega_s$.

vation of the equilibrium, indicating stability. (Admittedly, there is 1% decrease of σ_p from its initial value, but a later improvement in the PF interpolation algorithm [9] gave a nearly constant σ_p at this current.) At $N = 1.64 \cdot 10^{10}$ we see a slowly developing instability, indicating a current close to threshold, while at $N = 1.74 \cdot 10^{10}$ there is a pronounced instability evolving toward a pattern of quadrupole-type oscillations with constant amplitude. The bunch length σ_q of course shows similar behavior.

At still higher current the envelope of the quadrupole oscillations shows a sawtooth behavior. Figure 7 shows σ_q at $N = 2.99 \cdot 10^{10}$. Figure 8 displays snapshots of the charge distribution in the sawtooth mode at various times. Figure 9 shows an analogous but not directly comparable calculation by Bane and Oide [17], using the macroparticle method rather than VFP. This was for an earlier version of the damping ring vacuum chamber, and was done with $3 \cdot 10^5$ macroparticles and the damping time reduced artificially by a factor of 10. The simulation shows much higher noise than our VFP calculation, but it was done years in advance of our work, and gave a qualitatively similar result.

To compare to experiment we try to simulate the oscilloscope trace from a BPM signal processed through a diode which makes an analog squaring of the signal [2, 16]. We had to assume a frequency-independent impedance of the BPM system. A measurement of that im-

FIGURE 7. Time evolution of the dimensionless bunch length σ_q, for bunch population $N = 2.99 \cdot 10^{10}$. The time unit is one synchrotron period. A fairly clear periodic behavior sets in at about 2.5 damping times (500 synchrotron periods).
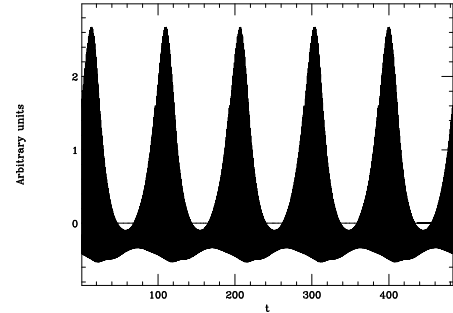

FIGURE 10. Simulated oscilloscope trace for $N = 2.99 \cdot 10^{10}$, in arbitrary units. The time unit is one synchrotron period. The straight line gives the mean value of the plotted data, zero as it ought to be.

pedance is possible, but has not been made. The predicted trace is shown in Figure 10; it is qualitatively similar to the corresponding experimental result, the third trace from the top of Figure 1.
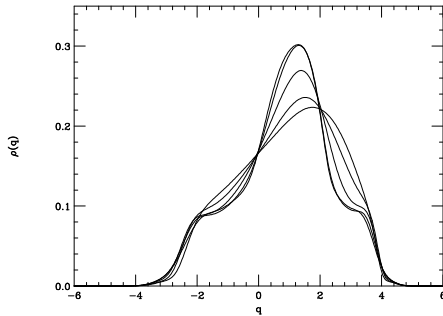
FIGURE 8. Typical snapshots of the charge distribution for bunch population $N = 2.99 \cdot 10^{10}$. The interval between snapshots is 6 synchrotron periods.
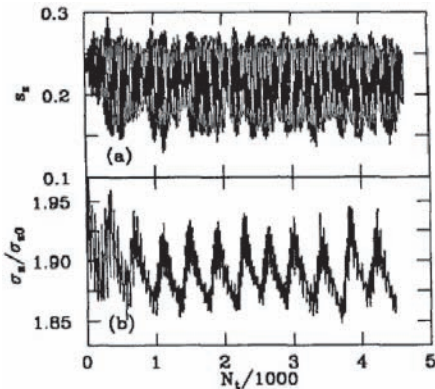
FIGURE 9. Macroparticle simulation of SLC damping ring (old vacuum chamber) from Ref.[17]. The upper graph is the normalized third moment (skew) of the charge distribution for $N = 3.5 \cdot 10^{10}$ *vs.* number of turns N_t. The lower graph is the normalized r.m.s. bunch length for $N = 5 \cdot 10^{10}$.

In summary, the calculation is qualitatively successful in that it reproduces the observed sequence of behaviors

with increasing current: equilibrium $\rightarrow$ quadrupole-like oscillations with constant amplitude $\rightarrow$ sawtooth pattern in the envelope of quadrupole oscillations. Also, the predicted form of the oscilloscope trace resembles experiment. As reported in [2], the current threshold of instability ($N = 1.64 \cdot 10^{1}0$), the quadrupole frequency ($1.8\omega_s$), and the sawtooth period ($0.6t_d$) were in good agreement with experiment. The claim concerning the threshold may be revised in forthcoming work, however, since there was a mistake in scaling z-dependence of the wake field.

Experimentally, the sawtooth goes away at still higher current, and is replaced by a sextupole-like constant amplitude oscillation. In the simulation, the sawtooth persists at higher current, still with quadrupole oscillations. Presumably this failure is due to our poor knowledge of the wake field at short wavelengths.

BURSTS OF CSR IN THE NSLS-VUV

In this example, treated in [18], we use machine parameters of NSLS-VUV light source, with a wake field given by shielded CSR alone. Dynamics are such that the effectiveness of the shielding varies with time. The machine wake is ignored, and that is quantitatively wrong. Studies are underway to include at least a broad-band resonator wake [19]. We start with equilibrium state (here almost Gaussian), slightly perturbed in the most unstable mode as determined by linear coasting beam theory. We compute the ratio of coherent radiated power to incoherent power as a function of time. The result plotted in Figure 11 shows periodic bursts, in qualitative agreement with experimental data shown in Figure 3. The current threshold for bursting is higher than in experiments, but that may be partly due to neglect of the machine wake. Figure 12 gives the bunch length σ_q as a function of time, which displays a sawtooth pattern reminiscent of

the SLC case. Bursts in coherent power correlate with times of minimum bunch length, which in turn correlate with microbunching such as that shown in Figure 13. Microbunching is necessary to overcome shielding of CSR by the vacuum chamber.
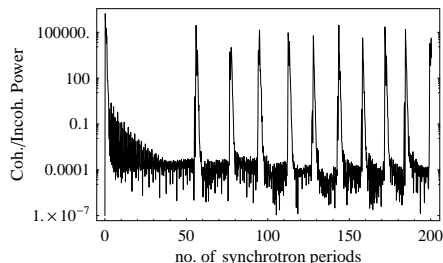

FIGURE 11. Coherent over incoherent power

A COMPACT STORAGE RING FOR X-RAY PRODUCTION

Our next example is a design for a small, fast cycling electron ring to produce X-rays by Compton scattering on a laser pulse stored in an optical cavity [20]. The ring circumference of only 6.3m is to maximize the collision frequency. Because of the small bending radius, the effect of CSR on beam stability is an issue. Because of the low energy, the damping time is effectively infinite, being much larger than the storage time. Parameters and details of our calculation are given in [20]. The collective force is from shielded CSR alone, and there are no FP terms since $t_d = \infty$. The integration begins with the equilbrium (which is conditioned mostly by the space charge force), slightly perturbed in the most unstable mode n=702, wavelength 2.2mm. We follow the phase distribution for a few synchrotron periods with high resolution.

The current threshold of instability (7.1 nC) agrees well with the coasting beam estimate, and is well above design requirements. Above threshold, small ripples in the charge distribution build up in a fraction of a period,
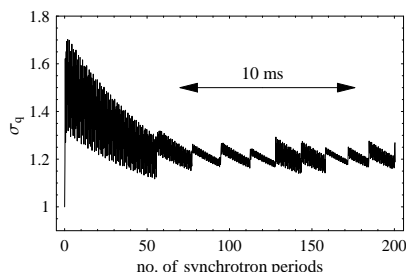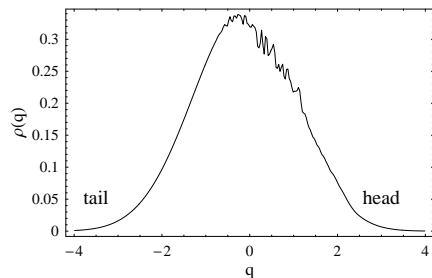

FIGURE 12. Bunch length vs. time

FIGURE 13. Bunch density with 'microbunching'

but then die out to produce a smoother distribution within two periods. This is seen in Figure 14 which shows the phase space distribution and the corresponding projection giving the charge distribution.

The quick smoothing of the phase distribution suggests a physical mechanism for the CSR bursts of the previous section. Small ripples in a short bunch build up through instability due to CSR, since the size of ripples is below the shielding cut-off. There is a corresponding burst of radiation, but it has limited duration, because of the rapid smoothing out of ripples due to the nonlinear, time dependent collective force. There is an attendant bunch lengthening, and disappearance of all structures below the shielding cutoff in size. Damping and diffusion from incoherent radiation then gradually decrease the bunch length until the conditions for the instability are restored, and another burst occurs.

CONCLUSIONS AND OUTLOOK

We have improved the theory of longitudinal bunch instabilities in several ways: (a) by providing a more efficient method to determine the equilibrium distribution; (b) by giving a better formulation of the linearized Vlasov equation for a bunched beam; (c) most importantly, by finding a simple technique for time-domain integration of the nonlinear Vlasov-Fokker-Planck equation. The latter has led to insights on interesting nonlinear phenomena such as the sawtooth mode and CSR in the bursting mode, and to some agreement with experiments.

There is further work to be done on the longitudinal problem in special circumstances, for instance for steady CSR achieved by a special machine setup [21], and for beam slicing experiments [22]. Also, it will be informative to do simulations for other machines such as DAΦNE in which the wake potential has been calculated carefully [23]. Algorithm development, including extensions to higher dimensional phase space, is of course prominent in our plans and current work. Single-pass CSR, as in bunch compressors, is an outstanding problem of current interest. There the question of micro-

bunching and the matter of reducing noise in simulations are big issues. We hope that the Vlasov PF method will be helpful in this regard, even though it is complicated by being in 4-D phase space with difficult issues concerning field computation and choice of meshes. [24].

ACKNOWLEDGMENT

REFERENCES

1. L. D. Landau, J. Phys. USSR **10**, 25 (1946).
2. R. Warnock and J. Ellison, in *The Physics of High Brightness Beams*, (World Scientific, Singapore, 2000), also SLAC-PUB-8404 (2000).
3. R. Warnock and M. Venturini, Proc. 2003 Part. Accel. Conf., Portland, Oregon, paper RPPB061.
4. K. Oide and K. Yokoya, KEK Laboratory Report KEK 90-10 (1990); K. Oide, KEK 90-168 (1990), KEK 94-138 (1994).
5. G. R. Bart and R. L. Warnock, SIAM J. Math. Anal. **4**, 609 (1973).
6. R. Warnock, G. Stupakov, M. Venturini, and J. A. Ellison, Proc. 2004 Euro. Part. Accel. Conf., Luzern, Switzerland.
7. N. I. Muskhelishvili, *Singular Integral Equations*, (Noordhoff, Groningen, 1953).
8. E. Sonnendrücker, J. Roche, P. Bertrand, and A. Ghizzo, J. Comp. Phys. **149**, 201 (1999); F. Filbet and E. Sonnendrücker, Comput. Phys. Commun. **150**, 247 (2003).
9. T. Nakamura and T. Yabe, Comput. Phys. Commun. **120**, 122 (1999).
10. C. Z. Cheng and G. Knorr, J. Comp. Phys. **22**, 330 (1976).
11. R. Warnock and J. Ellison, Phys. Rev. ST - Accel. Beams **6**, 104401 (2003).
12. A. Sobol, Ph.D. thesis, University of New Mexico, in preparation; A. Sobol and J.A. Ellison, AIP Conf. Proc. **693**, 2003.
13. M. Vogt, J. Ellison, T. Sen, and R. Warnock, Proc. of Workshop on Beam-Beam Effects in Circular Colliders, Fermilab, June 25-27, 2001, FERMILAB-Conf-01/390-T, p.149.
14. N. Towne, Phys. Rev. ST Accel. Beams 4, 114401 (2001)
15. G. Bassi, *Analytical and Numerical Studies of Stochastic Effects in Beam Dynamics*, Ph.D. thesis, University of Bologna, 2003.
16. B. V. Podobedov, *Saw-Tooth Instability Studies at the Stanford Linear Collider Damping Rings*, Stanford Ph.D. thesis, 1999, SLAC-R-543.
17. K. L. F. Bane and K. Oide, SLAC-PUB-6216, 1993.
18. M. Venturini and R. Warnock, Phys. Rev. Lett. **89**, 224802 (2002).
19. M. Salas, *A Numerical Study of the Vlasov-Fokker-Planck Equation with Applicaations to Particle Beam Dynamics*, M.S. thesis, University of New Mexico, 2005.
20. M. Venturini, R. Warnock, and R. Ruth, Phys. Rev. ST Accel. Beams **8**, 014202 (2005).
21. F. Sannibale, J. M. Byrd, Á. Loftsdóttir, M. Venturini, M. Abo-bakr, J. Feikes, K. Holldack, P. Kuske, G. Wüstefeld, H.-W. Hübers, and R. Warnock, Phys. Rev. Lett. **93**, 094801 (2004).
22. A. Zholents and M. Zolotorev, Phys. Rev. Lett. **76**, 912 (1996); A. Zholents *et al.*, Proc. 1999 Part. Accel. Conf., New York, p. 2370; J. Byrd *et al.*, Proc. 2005 Part. Accel. Conf., paper RPAE066; S. Kahn, *ibid.*, paper TOAB007.
23. B. Spataro and M. Zobov, DAΦNE Technical Note G-64, 2005, INFN-LNF, Frascati.
24. R. Warnock, G. Bassi, and J. Ellison, Proc. 8th Int. Comp. Accel. Phys. Conf., St. Petersburg, Russia, 2004 (to be published in Nucl. Instr. Meth. Sci. Res.)
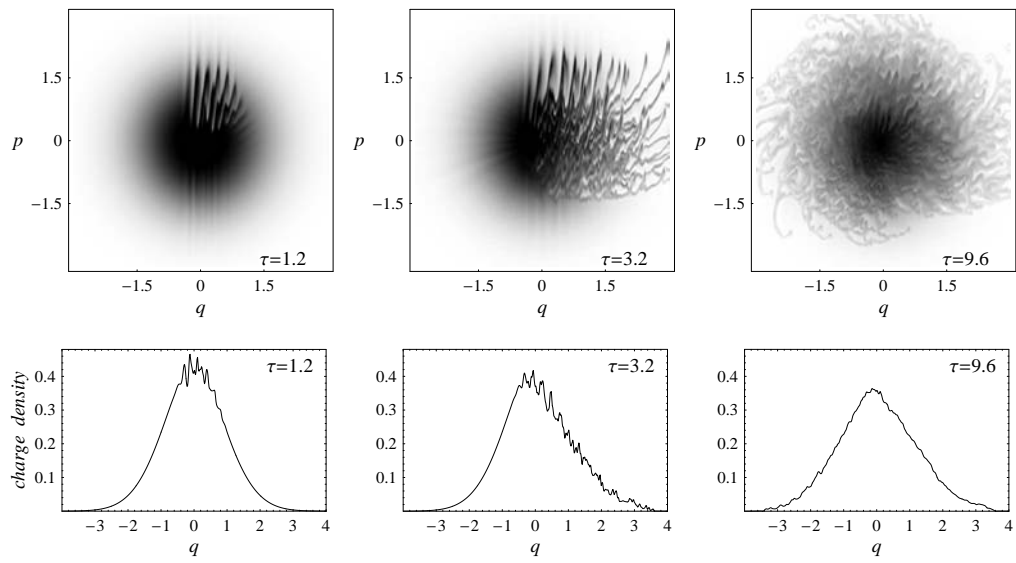
FIGURE 14. Time evolution of bunch under effect of CSR. Density plots in phase space (top row) and charge density (second row). Pictures are taken at (normalized) time $\tau = \omega_s t = 1.2, 3.2$, and 9.6. Instability initiated by a small perturbation with mode number $n = 702$ (wavelength $\lambda = 2.2$ mm). A unit of q corresponds to 1 cm.